

Brownian motion and shape fluctuations of single-layer adatom and vacancy clusters on surfaces: Theory and simulations

S. V. Khare* and T. L. Einstein†

Department of Physics, University of Maryland, College Park, Maryland 20742-4111

(Received 12 March 1996)

In recent observations of Brownian motion of islands of adsorbed atoms and of vacancies with mean radius R , the cluster diffusion constant D_c varies as R^{-1} and R^{-2} . From an analytical continuum description of the cluster's steplike boundary, we find a *single* Langevin equation for the motion of the cluster boundary, rather than three special cases. From this we determine D_c and the correlation function G_{sh} for fluctuations of the shape around an assumed equilibrium circular shape. In three limiting cases we find the scaling relations $D_c \sim R^{-\alpha}$ and, at early elapsed time t , $G_{sh} \sim t^{1/(1+\alpha)}$, where $\alpha = 1, 2, \text{ and } 3$, corresponding to the three generic surface mass-transport mechanisms of straight steps. We thereby provide a unified treatment of the dynamics of steps and of clusters. To check how well the continuum results describe clusters of the size in experiments, we perform Monte Carlo simulations of simple lattice gas models. Further, we estimate atomic diffusion parameters from the available experimental data on diffusion of large clusters. [S0163-1829(96)06239-X]

I. INTRODUCTION

Characterizing the mechanisms of atomic mass transport on surfaces is crucial to the understanding of many important processes, such as epitaxial growth. A notable manifestation of surface transport is the diffusion of single-layer clusters.¹⁻⁹ Of the few experimental studies relating the diffusion of clusters to their size, most have considered islands of no more than a few tens of atoms.^{2,3} For such small clusters, the details of the geometry of the structure and the interplay of the many energy barriers for single-atom diffusion lead to complicated size dependence, which can confound interpretation in terms of atomic processes. Using scanning tunneling microscopy (STM) Trevor *et al.*⁷ made one of the first direct observations of the diffusion of large vacancy and/or adatom clusters that are found on Au(111) in electrolyte solution by scanning tunneling microscopy (STM). These clusters were in the range of 2 to 10 nm in diameter. Trevor *et al.* observed that the cluster diffusion constant D_c decreases with the mean cluster radius R . Limited by their speed of observation, they were unable to characterize the decrease quantitatively. Recently, however, there have been three studies⁴⁻⁶ in which the diffusion constant of the islands D_c was measured as a function of large approximate island radius R . Morgenstern *et al.* (MRPC) (Ref. 4) studied single-layer vacancy clusters on Ag(111). Wen *et al.* (WCBET) (Ref. 5) studied adatom islands of Ag on Ag(001). Figuera *et al.*⁶ (FPOM) observed the motion of monolayer-deep vacancy islands on a Cu(111) surface covered with submonolayer amounts of Co. In all three experiments the number of vacancies (atoms) in the island ranged from 10^2 to 10^3 . For such sizes it becomes meaningful to describe the step edge position by a continuous variable. We derive results here that show how the same processes that govern step fluctuations in the continuum limit also produce adatom and vacancy cluster diffusion, deriving a general expression for the cluster-size dependence of the diffusion constant D_c of the cluster. Three limiting cases of this result were reported earlier in a Letter

by Bartelt and us.¹⁰ We also define and analyze an expression for a shape fluctuation correlation function; its scaling with time of observation of the clusters is found in the three limiting cases. These equilibrium fluctuations of steps on vicinal surfaces have been experimentally observed and analyzed in detail.¹¹⁻¹³ Their spatial and temporal correlations have also been characterized in the continuum limit using Langevin dynamics.¹⁴⁻¹⁸ From the similar, but more general, Langevin analysis of clusters that follows, we show how the various mechanisms of atomic transport across the surface underlie the Brownian motion of clusters. By comparison with experiment, we check that this unification of coarse-scale and atomic motion presents a fully consistent picture that is richer than the one obtained by scaling arguments^{4,5} alone or other theoretical attempts.¹⁹⁻²¹ We describe the continuum approach to the problem in Sec. II. The results of simulations are presented in Sec. III. We discuss the relevance of the results to experiment in Sec. IV and summarize in Sec. V.

II. LANGEVIN ANALYSIS

Consider an isolated adatom and/or vacancy island whose center of mass undergoes random fluctuations. We assume that the fluctuations are entirely the result of the motion of the boundary of the island, defined in cylindrical coordinates by

$$r = \tilde{r}(\theta, t), \quad (1)$$

where r and θ are the radial and azimuthal coordinates and t is the time. We assume that the lowest-energy configuration of the cluster is a circle of radius R . Under these conditions we can define a dimensionless variable $g(\theta, t)$ for the cluster boundary by

$$g(\theta, t) \equiv (\tilde{r}(\theta, t) - R)/R. \quad (2)$$

The diffusion constant D_c of the cluster is defined as

$$D_c \equiv \frac{\langle \vec{r}_{CM}^2(t) \rangle}{4t}, \quad (3)$$

where $\vec{r}_{CM}(t)$ is the position vector of the island's center of mass, and $\vec{r}_{CM}(0)$ is taken as the origin. Expanding the center of mass $\vec{r}_{CM}(t)$ to first order in $g(\theta, t)$, one can show that

$$D_c = \frac{R^2 \langle |g_1(t)|^2 \rangle}{t}, \quad (4)$$

where D_c is simplified by the Fourier representation $g(\theta, t) = \sum_n g_n(t) \exp(in\theta)$, with $n=0, \pm 1, \pm 2 \dots$. The restriction that $g_{-n}(t) = g_n^*(t)$ guarantees that $g(\theta, t)$ is real.

In analogy with the analysis for the single isolated step on a surface^{15,16,22} we define the cluster edge free energy as

$$F[\tilde{r}(\theta, t)] = \frac{\tilde{\beta}}{2R} \int_0^{2\pi} \left(\frac{d\tilde{r}}{d\theta} \right)^2 d\theta, \quad (5)$$

where the cluster-edge stiffness $\tilde{\beta}$ is assumed to be isotropic. It can be viewed as an "effective" surface tension of the cluster edge. Details of the derivation and how it differs from that of a straight step are sketched in the Appendix.

The thermodynamic definition of the chemical potential μ is $\mu \equiv \delta F / \delta N$, where N is the number of particles in the system. Similarly, Herring, Mullins, and others²³⁻²⁵ further defined a chemical potential that depends on surface geometry. Analogous to such a definition of the chemical potential μ_s for vicinal step edges,^{24,25} we assume that the chemical potential μ_s due to the cluster edge is given by

$$\mu_s = \left(\frac{\delta F}{\delta \tilde{r}} \right) \left(\frac{\delta N}{\delta \tilde{r}} \right)^{-1}, \quad (6)$$

where N is now the number of atoms and/or vacancies in the cluster and can be written in terms of the cluster area:

$$N = \int_0^{2\pi} \frac{\tilde{r}^2}{2\Omega} d\theta. \quad (7)$$

Here Ω is the area of the surface unit cell. Performing the functional minimizations in Eq. (6) (Ref. 22) from the forms of F given by Eq. (5) and N in Eq. (7), one gets, to linear order in $g(\theta, t)$,

$$\mu_s = - \frac{\Omega \tilde{\beta}}{R} \frac{d^2 g}{d\theta^2}. \quad (8)$$

This μ_s is the driving potential for the mass transport of the cluster, as shall be seen shortly through Eq. (9). Caveats regarding the definitions of F and μ_s are given in the Appendix. We apply the so-called radiation boundary condition in the adiabatic or quasistatic approximation. (See, e.g., Refs. 26-28.) We assume a steady-state concentration of adatoms on the upper and on the lower terraces of the cluster. Hence, the concentration does not depend explicitly on time. The diffusion equation for the adatom concentration $c(r, \theta)$ then becomes Laplace's equation. The incoming flux at a given point on the cluster edge consists of a normal component coming from the upper and the lower terrace and another contribution from motion along the cluster periphery. We

make the linear kinetic assumption, which means that this incoming flux is *linearly* proportional to the change in concentration on the upper and lower terrace due to the presence of the step edge. The first two terms on the left-hand side of the following equation describe the flux from the periphery and the terrace, respectively. The right-hand side indicates the attachment rate of this flux to the boundary; the proportionality constant Γ is the mobility. Thus, the boundary conditions for the concentration are given by

$$\begin{aligned} W_{\pm} \Omega R^{-2} D_{st} \frac{\partial^2 c(\tilde{r}^{\pm}, \theta)}{\partial \theta^2} + \Omega D_{su} \frac{\partial c(\tilde{r}^{\pm}, \theta)}{\partial r} \\ = \pm \Gamma_{\pm} \left[c(\tilde{r}^{\pm}, \theta) - \left(1 + \frac{\mu_s}{k_B T} \right) c_{su} \right]. \end{aligned} \quad (9)$$

For vacancy clusters, the right-hand side must be multiplied by an additional factor of -1 . The $+$ ($-$) region is outside (inside) the closed step, i.e., where $r > \tilde{r}$ ($r < \tilde{r}$). Γ_+ (Γ_-) is the step mobility due to the attachments onto the cluster edge from the $+$ ($-$) region. Similarly, $c(\tilde{r}^{\pm}, \theta)$ refer to the concentrations just outside (inside) the edge. With a_{\perp} an effective lattice constant in the radial direction perpendicular to the cluster edge, $W_+ = a_{\perp}$ for adatom clusters while $W_- = 0$; for vacancy clusters $W_+ = 0$ while $W_- = a_{\perp}$. It is assumed here that the motion along the cluster edge happens only along the lower terrace. If this were not the case, then $W_{\pm} = \pm a_{\perp}$ for adatom clusters and $W_{\pm} = \mp a_{\perp}$ for vacancy clusters. In this situation D_{st} in Eqs. (23), (26), (27), (31), and (32) should be replaced by $2D_{st}$. Ω is the area of the surface unit cell. D_{st} is the (tracer) diffusion constant of a single atom diffusing along the cluster [step] edge. D_{su} is the (tracer) diffusion constant of a single adatom diffusing on a flat (step-free) surface. c_{su} is the equilibrium surface concentration of adatoms far away from the cluster edge. The conservation of mass at the cluster edge implies that the velocity of the cluster edge should be proportional to the incoming flux from both terraces, combined. The incoming flux is given by the left hand side of Eq. (9). Thus using Eq. (9) the cluster edge velocity is given by

$$\begin{aligned} R \frac{\partial g(\theta, t)}{\partial t} = \Gamma_+ \left[c(\tilde{r}^+, \theta) - \left(1 + \frac{\mu_s}{k_B T} \right) c_{su} \right] \\ + \Gamma_- \left[c(\tilde{r}^-, \theta) - \left(1 + \frac{\mu_s}{k_B T} \right) c_{su} \right]. \end{aligned} \quad (10)$$

We solve the Laplace's equation for $c(r, \theta)$ in two dimensions with the boundary conditions of Eq. (9) and with other obvious restrictions such as the boundedness of $c(r, \theta)$, $c(0, \theta) = c(\infty, \theta) = c_{su}$, and $c(r, \theta + 2\pi) = c(r, \theta)$ and substitute it into Eq. (10) to get

$$\frac{\partial g(\theta, t)}{\partial t} = - \sum_{m=-\infty}^{\infty} \tau_m^{-1} g_m(t) e^{im\theta}. \quad (11)$$

Here τ_m^{-1} is given by

$$1/\tau_m = \left[\frac{c_{su}\Omega^2\tilde{\beta}|m|^3}{k_B TR^3} \left(\frac{D_{su} + \frac{|W_+|D_{st}|m|}{R}}{1 + \frac{D_{su}\Omega|m|}{\Gamma_+ R} + \frac{|W_+|D_{st}\Omega m^2}{\Gamma_+ R^2}} + \frac{D_{su} + \frac{|W_-|D_{st}|m|}{R}}{1 + \frac{D_{su}\Omega|m|}{\Gamma_- R} + \frac{|W_-|D_{st}\Omega m^2}{\Gamma_- R^2}} \right) \right]. \quad (12)$$

Equation (11) is a breakup of the cluster edge velocity into its Fourier components. Each term in the summation corresponds to a particular Fourier component with a characteristic relaxation time τ_m . To convert Eq. (11) into a Langevin equation, we add an appropriate noise term $\zeta(\theta, t) = \sum_n \zeta_n(t) \exp(in\theta)$, with $n=0, \pm 1, \pm 2 \dots$. We can easily solve the resulting equation for the Fourier components,

$$\frac{\partial g_n(t)}{\partial t} = -\frac{g_n(t)}{\tau_n} + \zeta_n(t), \quad (13)$$

to get

$$g_n(t) = e^{-t/\tau_n} \left[g_n(0) + \int_0^t e^{t'/\tau_n} \zeta_n(t') dt' \right]. \quad (14)$$

We choose the noise such that

$$\langle \zeta_n(t) \zeta_{-m}(t') \rangle = f_n \delta_{n,m} \delta(t-t'). \quad (15)$$

If one starts at time $t=0$ with a perfectly circular cluster, then the correlations of g at future time t are given by combining Eqs. (14) and (15):

$$\langle |g_n(t)|^2 \rangle = \langle g_n(t) g_{-n}(t) \rangle = \frac{f_n \tau_n (1 - e^{-2t/\tau_n})}{2}. \quad (16)$$

We note here that the right-hand side of Eq. (16) vanishes as required at $t=0$, when the cluster is perfectly circular. If we express the free energy due to the cluster edge, Eq. (5), in terms of $g_n(t)$'s, it follows from the equipartition of energy among the capillary modes $g_n(t)$ in equilibrium²⁹ that

$$\langle |g_n(t)|^2 \rangle = k_B T / (2\pi\tilde{\beta} R n^2). \quad (17)$$

Under these conditions

$$f_n = k_B T / (\pi\tilde{\beta} R \tau_n n^2). \quad (18)$$

This result with Eq. (12) determines the second-order noise correlations completely. When $t/\tau_1 \ll 1$ the exponential in Eq. (16) for the case $n=1$ can be expanded to first order in t . With Eq. (4) and Eq. (18) this gives

$$D_c = R^2 f_1 = k_B TR / (\pi\tilde{\beta} \tau_1). \quad (19)$$

The above result with Eq. (12) for $m=1$ gives the value of D_c for $t/\tau_1 \ll 1$. Now suppose that $t/\tau_1 \not\ll 1$. We argue that the diffusion constant remains the same as given above, based on the following reasoning. Let us write the center of mass position vector at some arbitrarily large time t_M , as

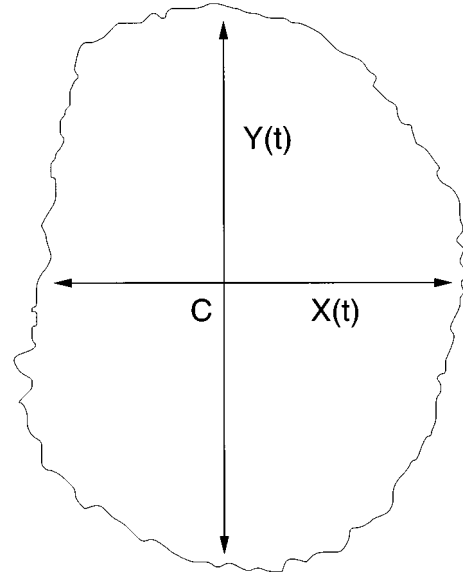


FIG. 1. Schematic representation of a vacancy cluster undergoing fluctuations of its boundary. C is the center of mass of the cluster at time t . $X(t)$ and $Y(t)$ are dimensions of the cluster in an orthogonal coordinate system passing through C , defined to be the origin.

$\vec{r}_{CM}(t_M) = \sum_{i=1}^M [\vec{r}_{CM}(t_i) - \vec{r}_{CM}(t_{i-1})]$, where $0 \equiv t_0 < t_1 < t_2 < \dots < t_{M-1} < t_M$. We assume that $\vec{r}_{CM}(0)$ is the origin. Hence, we get

$$\begin{aligned} \frac{\langle \vec{r}_{CM}^2(t_M) \rangle}{4t_M} &= (4t_M)^{-1} \left(\sum_{i=1}^M \langle [\vec{r}(t_i) - \vec{r}(t_{i-1})]^2 \rangle \right. \\ &\quad + 2 \sum_{i=1}^M \sum_{j=i+1}^M \langle [\vec{r}(t_i) - \vec{r}(t_{i-1})] \cdot [\vec{r}(t_j) \\ &\quad \left. - \vec{r}(t_{j-1})] \rangle \right). \quad (20) \end{aligned}$$

We choose the time intervals such that $(t_i - t_{i-1})/\tau_1 \ll 1$ and also $M \gg 1$. We assume that displacements at different times are uncorrelated if separated by time intervals greater than a few atomic events. Then the contribution from the double summation becomes negligible compared to the first sum. Thus even at long times, D_c is given by the first sum, which evaluates to the ‘‘short times’’ expression in Eq. (19).

Having found D_c , we now calculate the shape fluctuations of the cluster. We define a shape fluctuation correlation function $G_{sh}(t, t')$ with $t' - t > 0$ as

$$G_{sh}(t, t') = \langle [\delta(t) - \delta(t')]^2 \rangle, \quad (21)$$

where $\delta(t) \equiv X(t) - Y(t)$. $X(t)$ and $Y(t)$ are defined pictorially in Fig. 1 and are evaluated as $X(t) = \vec{r}(0, t) - \vec{r}(\pi, t)$ and $Y(t) = \vec{r}(\pi/2, t) - \vec{r}(3\pi/2, t)$. We assume that we begin with a cluster for which the fluctuations of its boundary have already reached their equilibrium value given by Eq. (17) at time $t=0$. One gets, after some algebra and using $\tau_{-m} = \tau_m$, the relation

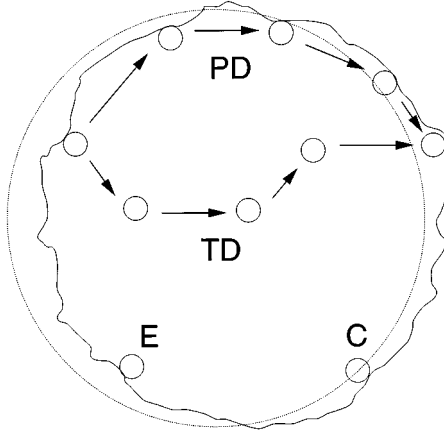


FIG. 2. Schematic representation of the three types of diffusion mechanisms considered here. The large circle represents the average circular shape of a vacancy island on the surface. The solid line shows a fluctuation giving rise to a shift of the center of mass to the right. Two paths of the adatom motion marked TD (for terrace diffusion) and PD (for periphery diffusion) for the same initial and final position of the migrating atom are depicted with arrows. The atoms marked E and C represent the third mechanism of evaporation and condensation from the vacancy edge. The atom marked C is one that has just condensed onto the vacancy edge. The one marked E is the one that will soon evaporate from the edge.

$$G_{sh}(t, t') = \frac{16Rk_B T}{\pi\tilde{\beta}} \sum_{m=0}^{\infty} \left[\frac{1 - \exp(-(t' - t)/\tau_{2m+1})}{(2m+1)^2} \right]. \quad (22)$$

Equations (11), (12), (19), and (22) hold in general, i.e., when mass transport on the surface takes place along the cluster boundary as well as on the terraces. As is the case of ‘‘straight’’ steps (or the decay of surface profiles^{25,30}), three limiting cases are of special interest, corresponding to three distinct mechanisms of mass transport occurring at the cluster boundary. These limiting cases lead to the scaling of D_c with R and of $G_{sh}(t, t')$ with the elapsed time $t' - t$. These are illustrated schematically in Fig. 2 and their description is now given.

Periphery or edge diffusion (PD). When the mass transport occurs only along the edge of the boundary (and the number of atoms and/or vacancies in the island are preserved), we take $D_{su} = 0$. Also if the rate limiting step is diffusion along the boundary, then the term of unity in the denominator of Eq. (12) is taken to be the dominant term to get $1/\tau_n$ as

$$1/\tau_n = D_{st}c_{st}\Omega^2\tilde{\beta}n^4/(k_B TR^4), \quad (23)$$

where c_{st} is defined by $c_{st} \equiv c_{su}a_{\perp}$.

Terrace or surface diffusion (TD). Suppose that the boundary of the island can emit atoms very rapidly, but atoms diffuse away slowly from the boundary. The rate-limiting step in mass transport is then the diffusion on terraces. We take $D_{st} = 0$ with the term of unity in the denominator to be dominant to get $1/\tau_n$ as

$$1/\tau_n = 2D_{su}c_{su}\Omega^2\tilde{\beta}|n|^3/(k_B TR^3). \quad (24)$$

Furthermore, if carriers attach and/or detach from only one side, as is believed to be the case^{4,8} for Ag(111), one must remove the factor of 2 in Eq. (24). This scaling behavior has also been derived analytically from a different atomistic perspective by Van Siclen¹⁹ and also by Soler,³¹ for ‘‘correlated’’ evaporation-condensation.

Evaporation and condensation limited diffusion (EC). In this case the rate-limiting step for mass transport is the random attachment and/or detachment of adatoms (or vacancies) at the edge of the boundary (from and/or to a reservoir of adatoms on the terraces or, in principle, in the vapor). Then one can ignore the constant term in the denominator and define $\Gamma = (c_{su}\Omega(\Gamma_+ + \Gamma_-))/2$ to get $1/\tau_n$ of the form

$$1/\tau_n = \Gamma\tilde{\beta}n^2/(k_B TR^2), \quad (25)$$

where Γ , the step mobility, is proportional to the rate of random attachments (detachments).^{13,29}

The cases PD and EC are examples of models B and A, respectively, in dynamical critical phenomena.³² From Eqs. (19), (20), (23), (24), and (25) we see that in all three cases the diffusion constant D_c of the island or cluster is given by a relation of the form

$$D_c = D_{c0}R^{-\alpha}, \quad (26)$$

where $\alpha = 3, 2, 1$ for the case of PD, TD, and EC, respectively, and the corresponding expressions for D_{c0} are $D_{st}c_{st}\Omega^2/\pi$, $2D_{su}c_{su}\Omega^2/\pi$, and Γ/π .

Also the summation for $G_{sh}(t, t')$ can in these three limiting cases be converted into an integral by taking a large- R limit, giving rise to the scaling with $t' - t$. This yields

$$G_{sh}(t, t') = \frac{8}{\pi} [\Gamma(\alpha/(1+\alpha))] \times (k_B T/\tilde{\beta})^2 [\pi D_{c0}(\tilde{\beta}/k_B T)^{\alpha+2} |t' - t|]^{1/(1+\alpha)}. \quad (27)$$

[Note that the Γ appearing in Eq. (27) is a gamma function and not the mobility.] This large- R leading term corresponds to an early-time expansion; there is no equivalent to Eq. (20) by which it can be extended to later times. Gruber³³ found an expression for D_c corresponding to Eq. (26) for a *three-dimensional* void diffusing in a solid in the case of PD. Generalizing his arguments to two dimensions, we obtained the same expression for D_c as in our Langevin analysis of the PD case. In the three limiting cases, the Langevin equations for the velocity of the cluster boundary also simplify considerably. The expressions for τ_n from Eqs. (23), (24), and (25) can be substituted back into Eq. (13) and the inverse Fourier transform performed. In these limits Eq. (13) then takes the real space form,

$$\frac{\partial g(\theta, t)}{\partial t} = \mathcal{F}[g(\theta, t)] + \zeta(\theta, t), \quad (28)$$

where $\mathcal{F}[g(\theta, t)]$ is in general a functional of $g(\theta, t)$. The second-order noise correlations of $\zeta(\theta, t)$ can also be calculated by taking the inverse Fourier transform of Eq. (15) with the use of Eqs. (18), (23), (24), and (25).

For the case of EC,

$$\mathcal{F}[g(\theta, t)] = \frac{\Gamma \tilde{\beta}}{R^2 k_B T} \frac{\partial^2 g(\theta, t)}{\partial \theta^2} \quad (29)$$

with

$$\langle \zeta(\theta, t) \zeta(\theta', t') \rangle = \frac{\Gamma}{\pi R^3} \delta(\theta - \theta') \delta(t - t'). \quad (30)$$

For the case of PD, the conservation of carriers along the steps adds the operator $-\partial^2/\partial\theta^2$, so that

$$\mathcal{F}[g(\theta, t)] = \frac{-D_{st} c_{st} \Omega^2 \tilde{\beta}}{R^4 k_B T} \frac{\partial^4 g(\theta, t)}{\partial \theta^4} \quad (31)$$

with

$$\langle \zeta(\theta, t) \zeta(\theta', t') \rangle = \frac{D_{st} c_{st} \Omega^2}{\pi R^5} \delta''(\theta - \theta') \delta(t - t'). \quad (32)$$

For the case of TD, \mathcal{F} is nonlocal:

$$\mathcal{F}[g(\theta, t)] = \frac{D_{su} c_{su} \Omega^2 \tilde{\beta}}{\pi R^3 k_B T} \int_0^{2\pi} \left[\frac{\partial^2 g(\phi, t)}{\partial \phi^2} \right]_\phi S(\theta - \phi) d\phi \quad (33)$$

with

$$\langle \zeta(\theta, t) \zeta(\theta', t') \rangle = \frac{-2D_{su} c_{su} \Omega^2}{\pi R^4} S(\theta - \theta') \delta(t - t'). \quad (34)$$

Here $S(x)$ is given by

$$S(x) = \frac{1 - \cosh(\omega) \cos(x)}{[\cosh(\omega) - \cos(x)]^2} \quad (35)$$

and ω is a convergence factor to account for the nonvanishing lattice constant: $\omega \approx a_{\parallel}/R$, where a_{\parallel} is a lattice constant along the cluster boundary.

Since we have produced a general formalism not limited to the three special cases, we can examine the crossover from one regime to another. The crucial question is how narrow the crossover regions are, and thus how likely one is to observe them in experiments. Defining $R_{su} \equiv D_{su} \Omega / \Gamma_+$ and $R_{st} \equiv (a_{\perp} D_{st} \Omega / \Gamma_+)^{1/2}$, and using Eqs. (12) and (19), we write for an adatom cluster where mass transport is only in the lower terrace,

$$D_c = \frac{c_{su} \Omega \Gamma_+}{\pi R} \left(\frac{(R_{su}/R) + (R_{st}/R)^2}{1 + (R_{su}/R) + (R_{st}/R)^2} \right). \quad (36)$$

The expression in large parentheses is essentially identical to that presented in an appendix by Bonzel and Mullins²⁵ in conjunction with the straightening of an isolated step.³⁴ The effective exponent α defined by

$$\alpha(R) \equiv - \frac{\partial \ln D_c}{\partial \ln R} \quad (37)$$

can be written as

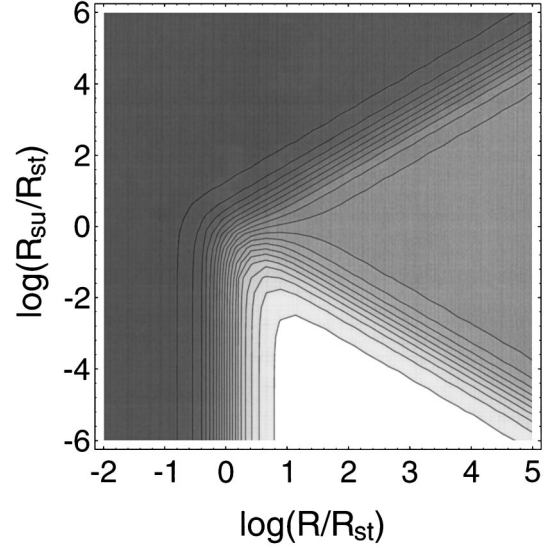


FIG. 3. Contour plot, with gray-scale shading, of the effective exponent $\alpha_{\text{eff}} \equiv -\partial \ln D_c / \partial \ln R$ as a function of the common logarithms \log_{10} , of R/R_{st} and R_{su}/R_{st} . Note that plateaus at the limiting-case, integer values 1 (gray), 2 (light gray), and 3 (white)—indicative of EC, TD, and PD, respectively—consume most of the parameter space; the crossover regions are rather narrow.

$$\alpha(R) = 2 + \left(\frac{1}{1 + (R/R_{st})(R_{su}/R_{st})} \right) - \left(\frac{2 + (R/R_{st})(R_{su}/R_{st})}{1 + (R/R_{st})(R_{su}/R_{st}) + (R/R_{st})^2} \right). \quad (38)$$

Hence, if $R \ll \max(R_{st}, R_{su})$, then $\alpha = 1$. If $R \gg \max(R_{su}, R_{st}^2/R_{su})$, then $\alpha = 2$. If $R_{st} \ll R \ll R_{st}^2/R_{su}$, then $\alpha = 3$. In principle, then, for a large enough cluster one should always find $\alpha = 2$, although this may well be unphysically large. The contour plot of α in Fig. 3 illustrates all these ideas and demonstrates that the crossover region occupies a rather narrow portion of parameter space and so is unlikely to occur in an experiment. Moreover, if it does, one should see noticeable changes in the effective exponent as R is increased. Good scaling with $\alpha \neq 1, 2, 3$ for over a decade suggests either experimental problems or physics beyond what is discussed in our analysis.

III. MONTE CARLO SIMULATIONS

The results of the continuum analysis demonstrate that the exponent α is a signature of the microscopic mechanisms of mass transport involved in the diffusion of the island. To check how these results appear in lattice systems with realistic dimensions, we also performed Monte Carlo simulations of three simple lattice-gas models of the three types of mass transport. The goal in these simulations was not to replicate any real system; instead we formulated simple models tailored to exhibit the three kinds of behavior, and then tested (i) whether the appropriate scaling was achieved and (ii) if the prefactor was the predicted transport coefficient. The latter aspect involved computing this coefficient in

the same model from a different perspective, by applying an external force and observing the response.

We used the standard Metropolis algorithm³⁵ on a square lattice with an (attractive) nearest-neighbor (NN) energy $-\epsilon$. Square lattices of dimensions $(L+40) \times (L+40)$ were studied. An initially square vacancy cluster of dimensions $L \times L$ was made by removing atoms around the center of the lattice (so $R=L/\sqrt{\pi}$). The sides of this cluster were chosen parallel to those of the larger square. In all three models L was chosen to be 10, 20, 40, and 80 atomic spacings. Data were not taken until the energy of the cluster had dropped to near its steady-state value, implying that the shape had equilibrated.

In the model for PD, Kawasaki dynamics [i.e., single-atom hops to a neighboring (vacant) site]³⁴ was used with the restriction that adatoms were allowed to diffuse only along the edge of the island via next-nearest-neighbor (NNN) exchange between a vacancy and an adatom. The temperature was set at $T=0.6\epsilon/k_B$, high enough so that the equilibrium shape of the cluster was nearly circular and so that adatoms had good mobility, but well below what would be the roughening temperature in an SOS model with the same ϵ . For present purposes we define an isolated adatom (vacancy) site as one which has all four NN sites empty (occupied by atoms). On a perfectly straight step, a NN hop of an edge atom (by necessity normal to the step) causes the formation of an isolated vacancy and an isolated adatom. This process costs an energy 3ϵ and hence is very slow. If the isolated adatom now hops along the edge to remove the isolated vacancy-adatom pair just generated, then it can do so with unit probability since the energy decreases (by ϵ). However, if the isolated adatom created does not hop along the edge before the vacancy penetrates the bulk, then we get bulk vacancy diffusion, which is prohibited in PD. (If an isolated vacancy were created, its hops in the surrounding area would happen with unit probability since they involve no energy change.) Also, most atoms on an equilibrated vacancy-island edge can make NNN hops but not NN hops without generating an isolated vacancy. The exclusively NNN-hop dynamics avoids these problems of very slow PD diffusion with NN hops and penetration of isolated vacancies into the bulk.³⁶ Any NNN hop which creates an isolated vacancy is also explicitly forbidden. So long as the diffusion is restricted to the periphery and is local, the exponent α should be independent of the specific choice of dynamics.

In the model for TD, the lattice gas Hamiltonian was slightly modified so that the energy of an isolated adatom on the terrace within the vacancy island was assigned an energy of ϵ rather than 4ϵ . The modification allows the vacancy cluster edge to emit atoms very rapidly, thereby facilitating adatom motion across the vacancy island. An initial density of adatoms in the vacancy of about 5% was introduced to reduce the time needed for equilibration. Kawasaki dynamics³⁵ was again used, but now diffusion of adatoms was allowed only via nearest-neighbor exchange between a vacancy and an adatom. Furthermore, single vacancies were not allowed to break away from the vacancy cluster, thus preventing its breakup into parts.³⁷ The temperature was set at $T=0.5\epsilon/k_B$.

In the model for EC, Glauber dynamics (i.e., removal or addition of single atoms) was used with random attachment

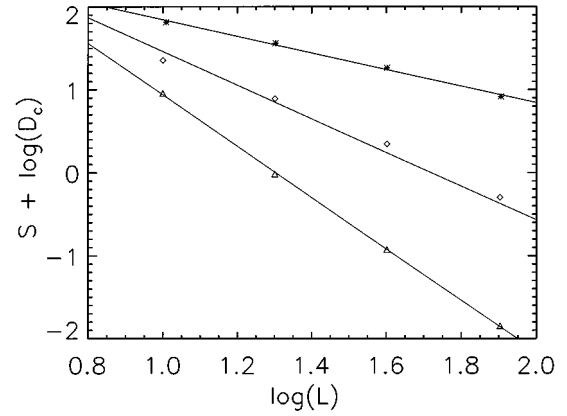


FIG. 4. Log-log plot (with common logarithms \log_{10}) of D_c vs L obtained from simulations of the three cases: EC (asterisks), TD (diamonds), and PD (triangles) is shown along with the best linear fits. $L=R\sqrt{\pi}$ is the linear dimension of the initial square shape of the vacancy. D_c is the diffusion constant of the cluster defined by Eq. (3). The arbitrary constant S shifts the y intercepts to allow display of all three cases together.

and/or detachment of adatoms allowed only along the edge of the island, at $T=0.6\epsilon/k_B$. In this dynamics the number of vacancies in the cluster fluctuates. For each value of L , the chemical potential of the reservoir was adjusted so that the mean number of vacancies comprising the cluster remained approximately the same as in the initial square configuration.

From the vacancy island simulations, plots of $\log_{10}D_c$ versus $\log_{10}L$ were made in all the three cases. These plots with their best linear fits are shown in Fig. 4. The slopes of the linear fits gave the three values of $\alpha=3.1$, 2.03, and 0.97, respectively. These values confirm the predictions of the Langevin analysis and the correspondence of the mass-transport mechanisms with the different values of α . The y intercepts of these fits gave the values of D_{c0} , which in turn give D_{st} , D_{su} , and Γ in the three cases. Plots of $\log G_{sh}(t,t')$ versus $\log(t'-t)$ were also made. These plots with their best linear fits are shown in Fig. 5. The slopes

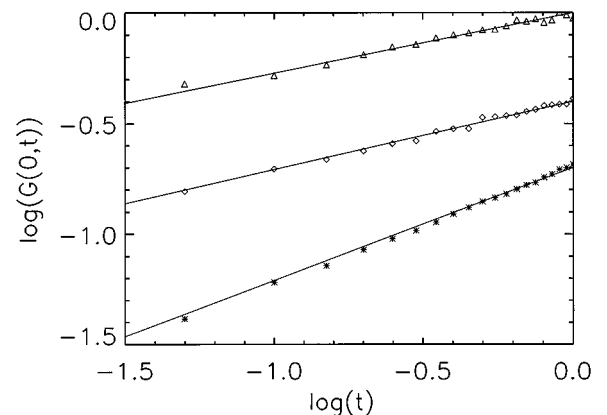


FIG. 5. Log-log plot [with common logarithms (\log_{10})] of $G_{sh}(0,t)$ vs t , both in arbitrary units. The triangles (PD), diamonds (TD), and asterisks (EC) are the data from Monte Carlo simulations. The solid lines are the best linear fits. The slopes are close to the predicted values $1/4$, $1/3$, and $1/2$, respectively. See text for details.

were 0.26, 0.31, and 0.51 for the PD, TD, and EC cases, respectively, corresponding very well with the continuum Langevin analysis predictions of 1/4, 1/3, and 1/2.

One can deduce $D_c \propto R^{-\alpha}$ from scaling arguments (cf. Sec. V). Thus, to corroborate our physical picture, it is important to be able to calculate the prefactors independently to verify that we are actually obtaining the relevant atomistic diffusion constants D_{st} , D_{su} , and Γ/a_{\parallel} in the prefactors. a_{\parallel} is a lattice constant along the step. In each case, to check the derived value of D_{c0} , we used the same Hamiltonians and dynamics, but instead of considering clusters, we applied a weak potential gradient \mathbf{F} to straight steps (for PD and EC) or a flat terrace with adatoms (for TD) to compute the constant diffusion constant D_{st} , Γ/a_{\parallel} , or D_{su} , respectively. The average velocity \bar{v} of the diffusing species was calculated as a function of \mathbf{F} , and the carrier diffusion constant obtained by applying the Einstein-Nernst relation $D = k_B T |\bar{v}|/|\mathbf{F}|$. For PD, \mathbf{F} was applied along (parallel to) the initial straight edge of a step with width $w=40$. For the TD case, \mathbf{F} was applied along one direction of a flat step-free square terrace with an adatom density c_{su} . For EC, \mathbf{F} was applied perpendicular to an initial straight step of width $w=40$; in this case \bar{v} refers to the average velocity of the whole step. The three diffusion constants D_{st} , D_{su} , and Γ/a calculated from the set of simulations with \mathbf{F} agreed to within 25% with their values obtained from the y intercepts (D_{c0}) in Fig. 4. The vacancy islands are finite in size. Also the Langevin analysis was done only to first order in g . Considering this finite size effect of the simulations and the linear approximation in the Langevin approach, we see that the agreement between diffusion constants obtained in the two ways is good. This agreement supports the appropriateness of the Langevin analysis of the simulations and, by implication, of the physical systems.

In a separate (Kawasaki³⁵ type) simulation, at each time step we removed an atom from one position along the boundary and immediately reattached it to the boundary at a random (with respect to the azimuthal angle) position, so that area is constantly conserved: $\oint \zeta(\theta, t) d\theta = 0$. The resulting log-log plot had a slope of 1.97. However, this straightforward Monte Carlo approach assumes random sampling of periphery sites with (fixed) time interval. In fact, as the periphery grows, the chance of a move per site should stay constant, so the chance of a move per time should be proportional to the circumference, leading to another factor of R . Hence $\alpha=0.97$, as for EC (see Ref. 38). For small adatom islands (but not vacancy pits) another diffusion mechanism is possible on such faces, more generally on $\{111\}$ fcc or $\{0001\}$ hcp faces with adsorption in either threefold site. Here diffusion can occur rapidly by the passage through the island of a dislocation line between domains in each of the two kinds of sites.³⁹

For PD diffusion WCBET (Ref. 5) cite values of α from early simulations^{40,41} in the range of 3 to 4. In these simulations the number of single atoms and/or vacancies in the islands was less than 10^2 . We believe that these values should converge to $\alpha=3$ for larger island sizes. WCBET (Ref. 5) also present heuristic arguments for obtaining the value of α for EC and PD diffusion. Stimulated by the work of Pimpinelli *et al.*,⁴² MRPC (Ref. 4) give a similar explanation of the phenomenon. Though this approach predicts the

correct exponents for the PD and TD mechanisms of diffusion, it does not readily provide precise quantitative information, such as the single atom diffusion constants and the step stiffness. While Shao *et al.*⁴³ have also studied the approach to the equilibrium shape of two-dimensional clusters on surfaces using Monte Carlo simulations, their emphasis is different. They probe the dependence of the time of equilibration of the cluster shape on the temperature and on the energy barriers for the motion of kink and corner atoms.

IV. ESTIMATES OF ENERGIES IN EXPERIMENT

This paper demonstrates that the phenomenon of surface diffusion of large islands can be viewed in a broader perspective: the cluster diffusion is a natural byproduct of the fluctuations of the bounding step. Observations of step fluctuations can then be used to make predictions about island diffusion. This approach also gives quantitative predictions for tracer diffusion constants from the observations of large island diffusion, as we illustrate for the three experiments at hand. The approximation that the ground state of the clusters is circular should be decent for temperatures at which the clusters diffuse, when they appear in STM images⁴⁻⁶ as quite rounded polygons. The presence or absence of corners should be particularly important for PD, which has not been observed to date in quantitative experiments involving adatom or vacancy islands. While the activation barriers estimated in what follows are crude, they provide some confidence that the physical picture underlying the preceding formalism is sensible. It is not feasible to extract more precise values without independent information about quantities such as c_{su} . Without independent information about the microscopics, any extracted energies should be viewed as effective rather than physical parameters.

In their study of adatom islands on Ag(001), WCBET (Ref. 5) found $\alpha=1$. Using $D_c \approx 10^{-3}$ nm²/s for an island of 100 atoms, we find $\Gamma/a \approx 1.8 \times 10^{-2}$ nm²/s for the diffusion of a step on Ag(001) at room temperature, where a is the surface lattice constant on the Ag(001) surface. Approximating the diffusion prefactor by 10^{11} nm²/s,² we obtain an activation energy of about 0.7 eV, which is a reasonable magnitude for a single atom detaching from a close-packed step on this surface.⁴⁴ In their study of vacancy clusters on Ag(111), MRPC (Ref. 4) found $\alpha=2$. Using $D_{c0} \approx 1.3$ nm⁴/s, we estimate the surface mass diffusion coefficient of Ag adatoms on Ag(111), $D_{su}c_{su} \approx 750$ s⁻¹. We then write $c_{su}\Omega = \exp(-E_f/k_B T)$, where E_f is the formation energy of an adatom in the vacancy clusters, and $D_{su} = 10^{11} \exp(-E_d/k_B T)$ nm²/s, where E_d is the diffusion barrier for an atom to hop on the Ag(111) surface. Hence, with $k_B T = 0.025$ eV we get $E_f + E_d = 0.53$ eV. If we assume $E_d = 0.1$ eV,⁴⁵⁻⁵¹ we get $E_f = 0.43$ eV, which has a reasonable order of magnitude.⁴⁴ Clearly, although the sum $E_f + E_d$ may be obtained from fitting the Langevin-derived expression to the experiment, the subsequent breakup into two energies is problematic. From Fig. 3(b) of FPOM,⁶ who also found $\alpha=2$, we use $D_{c0} \approx 4.2 \times 10^{-2}$ nm⁴/s to get $D_{su}c_{su} \approx 2.33$ nm²/s. Now as before we get $E_f + E_d = 0.61$ eV, a plausible estimate.⁴⁴

The extraction of microscopic energies from statistical data such as the above needs some caution. As noted

recently⁵² the energies so obtained are only as good as the correspondence of the model proposed for analysis of the data with the microscopic physical reality. In short, the conclusion of this section is that the numbers one extracts from the simplest analysis are of plausible magnitude.

V. DISCUSSION AND SUMMARY

There have been other approaches to this problem which predict the form of the scaling of the cluster diffusion constant D_c with its size. One of the first such arguments was given more than a decade ago by Binder and others^{53,54} in light of their simulation results of kinetic Ising spin models. Others have given similar arguments recently.^{4,5,20,21} They all essentially give dimensional scaling arguments to obtain the three values of $\alpha = 1, 2, 3$. In contrast to our approach, it is not clear how these results can be used to yield exact prefactors to extract microscopic energetics information from the experiment. An exact analytical expression for the scaling of the diffusion constant of the cluster D_c with its size is given by Ref. 19 for four distinct cases which yield $\alpha = 0, 1, 2$, and 3. Our expression for D_c given by Eq. (26) for the case of $\alpha = 1, 3$ agrees with that of Ref. 19. For the case $\alpha = 2$, our D_c differs from his by a factor of 2. This factor arises because he considers adatoms attaching and/or detaching from the cluster edge only from one side. Our unification of the previously well-characterized step-edge fluctuations and large-cluster diffusion is not so evident in any of these alternative approaches. Moreover, the scaling of the shape-fluctuations function with time emerges very naturally in our presentation. It is not so obvious how one would obtain this result from these alternative perspectives.^{4,5,19-21}

In all our work we have neglected any role of defects. In some cases, they evidently enhance the diffusion.⁶ More often we expect them to hinder the motion and cause problems in comparing data for nearly straight and nearly circular steps on the same surface. At least on non-close-packed surfaces, the diffusion along close-packed step edges is typically much greater than across terraces. Nonetheless, the cluster motion may often be dominated by TD because the diffusing atom cannot readily move around corners. This barrier would likely be enhanced by impurities residing at corners. More generally, impurities can pin steps,⁵⁵ destroying locally the fluctuations that have dominated our attention in this work.

In summary, we have shown how the diffusion of large clusters is simply a corollary of the fluctuations of the cluster boundary. We have developed a general Langevin analysis of diffusion of large islands. In three limiting cases we can give detailed predictions for the scaling of the diffusion constant D_c with the mean radius R . Furthermore, we can define a shape correlation function and explore its scaling with the time of observation in these cases. The scaling exponents signify the rate-limiting mass-transport mechanism involved. With Monte Carlo simulations we have illustrated the predictions of this continuum analysis in these limiting cases for surface mass transport. Finally, we applied the analytical predictions to the experimental data available and extracted single-atom diffusion constants. This approach allows us to measure atomic diffusion constants from observations of large-island diffusion.

ACKNOWLEDGMENTS

This work was supported in part by NSF Grant No. DMR-91-03031. T.L.E. also gratefully acknowledges support by a Humboldt U.S. Senior Scientist Award, the hospitality of the IGV/KFA Jülich, and subsequent helpful correspondence with G. Rosenfeld. We thank in particular N. C. Bartelt for invaluable collaboration in the early part of this work, for helpful suggestions thereafter, and for comments on the manuscript. We also thank P. J. Feibelman for several suggestions and comments on the manuscript, H. van Beijeren for insightful arguments about diffusion, and B. H. Cooper, P. M. Duxbury, B. Krishnamachari, and J. P. Sethna for providing us with unpublished results and related comments. S.V.K. thanks S. Kodiyalam for helpful discussions throughout the course of this work. S.V.K. also thanks Professor J. M. Soler for clarifications on Ref. 31.

APPENDIX

As an alternative to Eq. (5), the exact definition of F can be written as

$$F[\tilde{r}(\theta, t)] = \int_0^{2\pi} [\tilde{r}^2 + \dot{\tilde{r}}^2]^{1/2} \beta(\phi(\theta)) d\theta, \quad (A1)$$

where β is the free energy per unit length of the cluster edge and the dot on \tilde{r} indicates differentiation with respect to θ . The angle $\phi(\theta)$ is the direction of the local normal to the cluster boundary at the point $(\tilde{r}(\theta), \theta)$, so that for a circle $\phi(\theta) = \theta$. In general, we find that

$$\phi(\theta) = \tan^{-1} \left[\frac{\tilde{r} \sin \theta - \dot{\tilde{r}} \cos \theta}{\tilde{r} \cos \theta + \dot{\tilde{r}} \sin \theta} \right]. \quad (A2)$$

Performing the functional minimizations in Eq. (6) using this definition of F of Eq. (A1), one obtains the exact result for μ given by

$$\mu = \frac{\Omega \tilde{\beta}(\phi) (-\tilde{r} \ddot{\tilde{r}} + 2\dot{\tilde{r}}^2 + \tilde{r}^2)}{\tilde{r}^3 [1 + (\dot{\tilde{r}}/\tilde{r})^2]^{3/2}}, \quad (A3)$$

where the stiffness $\tilde{\beta}(\phi)$ is defined as $\beta(\phi) + d^2\beta(\phi)/d\phi^2$. Now ignoring the nonlinear terms in $\dot{\tilde{r}}/\tilde{r}$ and suppressing the ϕ dependence of $\tilde{\beta}$ one gets

$$\mu = \frac{\Omega \tilde{\beta}(\tilde{r} - \ddot{\tilde{r}})}{\tilde{r}^2} \equiv \frac{\Omega \tilde{\beta}(1 + g - \ddot{g})}{R(1 + g)^2} \approx \frac{\Omega \tilde{\beta}}{R} (1 - \ddot{g} - g), \quad (A4)$$

to lowest order in g . The first term is simply an additive constant Gibbs-Thomson term⁵⁶ that is not important for studying cluster diffusion and just shifts the reference chemical potential. The second term is what is given in Eq. (8). The angular average of the third term is zero. Moreover, it gives rise to cluster size instability: it causes the cluster either to grow without bound or to evaporate completely.⁵⁷⁻⁵⁹ Experimentally the clusters are found to be stable over the time of observation. Hence we omit this third term.

- *Electronic address: khare@surface.umd.edu
- †Electronic address: einstein@surface.umd.edu
- ¹J. J. Métois, K. Heinemann, and H. Poppa, *Philos. Mag.* **35**, 1413 (1977).
 - ²G. L. Kellogg, *Phys. Rev. Lett.* **73**, 1833 (1994); *Surf. Sci. Rep.* **21**, 1 (1994).
 - ³S. C. Wang and G. Ehrlich, *Surf. Sci.* **239**, 301 (1990).
 - ⁴K. Morgenstern, G. Rosenfeld, B. Poelsema, and G. Comsa, *Phys. Rev. Lett.* **74**, 2058 (1995).
 - ⁵J. M. Wen, S.-L. Chang, J. W. Burnett, J. W. Evans, and P.A. Thiel, *Phys. Rev. Lett.* **73**, 2591 (1994).
 - ⁶J. de la Figuera, J. E. Prieto, C. Ocal, and R. Miranda, *Solid State Commun.* **89**, 815 (1994).
 - ⁷D. J. Trevor and C. E. D. Cidsey, *J. Vac. Sci. Technol. B* **9**, 964 (1990).
 - ⁸K. Morgenstern, G. Rosenfeld, and G. Comsa, *Phys. Rev. Lett.* **76**, 2113 (1996).
 - ⁹J. M. Wen, J. W. Evans, M. C. Bartelt, J. W. Burnett, and P.A. Thiel, *Phys. Rev. Lett.* **76**, 652 (1996).
 - ¹⁰S. V. Khare, N. C. Bartelt, and T. L. Einstein, *Phys. Rev. Lett.* **75**, 2148 (1995).
 - ¹¹L. Kuipers, M. S. Hoogeman, and J. W. M. Frenken, *Phys. Rev. Lett.* **71**, 3517 (1993); L. Kuipers, M. S. Hoogeman, J. W. M. Frenken, and H. Van Beijeren, *Phys. Rev. B* **52**, 11 387 (1995).
 - ¹²M. Poensgen, J. F. Wolf, J. Frohn, M. Giesen, and H. Ibach, *Surf. Sci.* **274**, 430 (1992); M. Giesen-Seibert, R. Jentjens, M. Poensgen, and H. Ibach, *Phys. Rev. Lett.* **71**, 3521 (1993), **73**, E911 (1993); M. Giesen-Seibert, F. Schmitz, R. Jentjens, and H. Ibach, *Surf. Sci.* **329**, 47 (1995).
 - ¹³N. C. Bartelt, J. L. Goldberg, T. L. Einstein, E. D. Williams, J. C. Heyraud, and J. J. Métois, *Phys. Rev. B* **48**, 15 453 (1993).
 - ¹⁴J. Villain, *J. Phys. (Paris) I* **1**, 19 (1991).
 - ¹⁵N. C. Bartelt, J. L. Goldberg, T. L. Einstein, and E. D. Williams, *Surf. Sci.* **273**, 252 (1992).
 - ¹⁶N. C. Bartelt, T. L. Einstein, and E. D. Williams, *Surf. Sci.* **312**, 411 (1994).
 - ¹⁷P. Wang, H. Pfnür, S. V. Khare, T. L. Einstein, E. D. Williams, W. W. Pai, and J. Reutt-Robey, *Bull. Am. Phys. Soc.* **41**, 189 (1996) and unpublished.
 - ¹⁸B. Blagojević and P. M. Duxbury (unpublished).
 - ¹⁹Clinton DeW. Van Siclen, *Phys. Rev. Lett.* **75**, 1574 (1995).
 - ²⁰D. S. Sholl and R. T. Skodje, *Phys. Rev. Lett.* **75**, 3158 (1995).
 - ²¹J. M. Soler, *Phys. Rev. B* **50**, 5578 (1994).
 - ²²W. W. Mullins, in *Metal Surfaces: Structure, Energetics and Kinetics*, edited by N. A. Gjostein and R. W. Roberts (Am. Soc. Metals, Metals Park, OH, 1963), p. 17.
 - ²³C. Herring, in *The Physics of Powder Metallurgy*, edited by W. E. Kingston (McGraw-Hill, New York, 1951); C. Herring, *J. Appl. Phys.* **21**, 437 (1950); C. Herring, in *Structure and Properties of Solid Surfaces*, edited by R. Gomer and C. S. Smith (University of Chicago Press, Chicago, 1952).
 - ²⁴W. W. Mullins, *J. Appl. Phys.* **28**, 333 (1957); **36**, 77 (1959).
 - ²⁵H. P. Bonzel and W. W. Mullins, *Surf. Sci.* **350**, 285 (1996).
 - ²⁶G. S. Bales and A. Zangwill, *Phys. Rev. B* **41**, 5500 (1990).
 - ²⁷J. W. Cahn and J. E. Taylor, *Acta Metall. Mater.* **42**, 1045 (1994).
 - ²⁸A. A. Chernov, *Modern Crystallography III* (Springer-Verlag, Berlin, 1984).
 - ²⁹P. Nozières, in *Solids Far From Equilibrium*, edited by C. Godrèche (Cambridge University Press, Cambridge, 1992), p. 1.
 - ³⁰H. P. Bonzel and E. Preuss, *Surf. Sci.* **336**, 209 (1995).
 - ³¹J. M. Soler, *Phys. Rev. B* **53**, R10 540 (1996).
 - ³²P. C. Hohenberg and B. I. Halperin, *Rev. Mod. Phys.* **49**, 435 (1977). In spite of some tantalizing similarities, E. D. Siggia (private communication) notes that TD is not an example of model C.
 - ³³E. E. Gruber, *J. Appl. Phys.* **38**, 243 (1967).
 - ³⁴Specifically, our D_{st} is their νD^s , and our D_{su} is their $2\nu D^t$, the extra factor of 2 in their case allowing carriers on both sides of the steps. Their ν is our Ω , while their Ω is the volume rather than the area per atom, so νh in their notation. Their m/Ω is our $\Gamma/k_B T$. Their R_{iso}^t/m is our R_{su} , while their R_{iso}^s/m is our R_{st}^2 . Again, in going from nearly straight to nearly circular steps, we replace q by n/R .
 - ³⁵K. Binder and D. W. Heermann, *Monte Carlo Methods in Statistical Physics* (Springer, Berlin, 1988).
 - ³⁶This dynamics also avoids the anomalous behavior at corners in a NN-hop dynamics on a square lattice. J. G. McLean, B. H. Cooper, and E. Chason, *Bull. Am. Phys. Soc.* **40**, 598 (1995).
 - ³⁷With greater difficulty one could maintain a vacancy cluster of fixed size by using a system of appropriate finite size, as discussed in detail by B. Krishnamachari, J. G. McLean B. H. Cooper, and J. P. Sethna (unpublished).
 - ³⁸We are grateful to Professor H. van Beijeren for pointing out the extra factor of R , correcting an error in Ref. 10. He argues that with each move, the center of mass shifts by a distance of order Rt/R^2 , where the denominator accounts for the ‘‘mass’’ of the cluster. Then using Eq. (20) and noting that the number of moves per time goes like R , he finds $\alpha=1$.
 - ³⁹J. C. Hamilton, M. S. Daw, and S. M. Foiles, *Phys. Rev. Lett.* **74**, 2760 (1995).
 - ⁴⁰H. C. Kang, P. A. Thiel, and J. W. Evans, *J. Chem. Phys.* **93**, 9018 (1990).
 - ⁴¹A. F. Voter, *Phys. Rev. B* **34**, 6819 (1986); *SPIE: Mod. Opt. Thin Films* **821**, 214 (1987).
 - ⁴²A. Pimpinelli, J. Villain, D. E. Wolf, J. J. Métois, J. C. Heyraud, I. Elkinani, and G. Uimin, *Surf. Sci.* **295**, 143 (1993).
 - ⁴³H. Shao, S. Liu, and H. Metiu, *Phys. Rev. B* **51**, 7827 (1995).
 - ⁴⁴From table 16 of Ref. 45 we get the energy for an atom to detach from a kink on a close-packed step on Ag(001) to be 0.605 eV. From table 5 of Ref. 45 we get the value of adatom formation energy on the Ag(111) surface to be ≈ 1.027 eV/2 ≈ 0.5 eV. Also from the same table a similar calculation for Cu yields 0.65 eV. The Co covered Cu(111) surface is expected to have a lower energy (Ref. 6) for adatom formation which compares well with what we find.
 - ⁴⁵P. Stoltze, *J. Phys. Condens. Matter* **6**, 9495 (1994).
 - ⁴⁶This value is comparable to that of about 0.06 eV computed by the embedded atom method (EAM) (Ref. 47) 0.064 eV computed by Stoltze (Ref. 45), and 0.12 eV calculated by Jones *et al.* (Ref. 48) both using different variations of effective medium theory (EMT). The value obtained by the DFT-LDA method by Boisvert *et al.* (Ref. 49) is 0.14, which is slightly higher. However, with atomic relaxations being properly included and gradient corrections to the LDA method included, this energy is expected (Ref. 50) to be reduced to about 0.1 eV, as we have assumed here. This is also in agreement with the experimental value of 0.097 eV obtained by Bromann *et al.* (Ref. 51).
 - ⁴⁷R. C. Nelson, T. L. Einstein, S. V. Khare, and P. J. Rous, *Surf. Sci.* **295**, 462 (1993); C. L. Liu, J. M. Cohen, J. B. Adams, and A. F. Voter, *ibid.* **253**, 334 (1991).
 - ⁴⁸G. W. Jones, J. M. Marcano, J. K. Nørskov, and J. A. Venables,

- Phys. Rev. Lett. **65**, 3317 (1990).
- ⁴⁹G. Boisvert, L. J. Lewis, M. J. Puska, and R. M. Nieminen, Phys. Rev. B **52**, 9078 (1995).
- ⁵⁰Private communications with P. J. Feibelman and with G. Boisvert.
- ⁵¹K. Bromann, H. Brune, H. Röder, and K. Kern, Phys. Rev. Lett. **75**, 677 (1995).
- ⁵²P. J. Feibelman, Phys. Rev. B **52**, 12 444 (1995).
- ⁵³K. Binder and M. H. Kalos, in *Monte Carlo Methods in Statistical Physics*, edited by K. Binder, Topics in Current Physics Vol. 7 (Springer-Verlag, Berlin, 1986), Chap. 6, and references therein; K. Binder and M. H. Kalos, J. Stat. Phys. **22**, 363 (1980).
- ⁵⁴M. Rao, M. H. Kalos, J. L. Lebowitz, and J. Marro, Phys. Rev. B **13**, 4328 (1976).
- ⁵⁵J. Ozcomert, W. W. Pai, N. C. Bartelt, and J. E. Reutt-Robey, Surf. Sci. **293**, 183 (1993).
- ⁵⁶Note that for high terrace densities (i.e., large c_{su}), a correction is needed to the Gibbs-Thomson formula, cf. B. Krishnamachari, J. G. McLean, B. H. Cooper, and J. P. Sethna (unpublished).
- ⁵⁷D. S. Sholl and R. T. Skodje, Physica A (to be published).
- ⁵⁸M. Zinke-Allmang, L. C. Feldman, and M. H. Grabow, Surf. Sci. Rep. **16**, 377 (1992).
- ⁵⁹J. G. McLean, B. Krishnamachari, D. R. Peale, E. Chason, J. P. Sethna, and B. H. Cooper (unpublished).